

Thermally Induced Sigmatropic Isomerization of Pseudosaccharyl Allylic Ether

A. Gómez-Zavaglia,^{†,‡} A. Kaczor,^{†,§} R. Almeida,^{†,||} M. L. S. Cristiano,^{||} M. E. S. Eusébio,[†]
T. M. R. Maria,[†] P. Mobili,[⊥] and R. Fausto^{*,†}

Department of Chemistry, University of Coimbra, P-3004-535 Coimbra, Portugal, Faculty of Pharmacy and Biochemistry, University of Buenos Aires, C. P. 1113 Buenos Aires, Argentina, Faculty of Chemistry, Jagiellonian University, Ingardena 3, 30-060 Krakow, Poland, Department of Chemistry and Biochemistry, FCT and CCMAR, University of Algarve, P-8005-039 Faro, Portugal, and Center for Research and Development in Food Cryotechnology (CIDCA), 1900 La Plata, Argentina

Received: December 19, 2008; Revised Manuscript Received: January 28, 2009

The thermally induced sigmatropic isomerization of the pseudosaccharyl allylic ether [3-(allyloxy)-1,2-benzisothiazole 1,1-dioxide; ABID] has been investigated by a multidisciplinary approach using temperature dependent infrared spectroscopy, differential scanning calorimetry, and polarized light thermomicroscopy, complemented by theoretical methods. Migration of the allylic system from O to N occurs in the melted ABID, and the thermally obtained 2-allyl-1,2-benzisothiazol-3(2*H*)-one 1,1-dioxide (ABIOD) starts to be produced at ca. 150 °C, in a process with an activation energy of ~ 92 kJ mol⁻¹. From kinetic data, a concerted [3,3'] sigmatropic mechanism is proposed. In the temperature range investigated, ABIOD was found to exhibit polymorphism. Cooling of the molten compound leads to the production of a metastable crystalline form, which upon annealing at room temperature might be transformed to the stable crystalline phase. ABID shows a single crystalline variety. Assignments were proposed for the infrared spectra of the observed neat condensed phases of the two compounds.

Introduction

Benzisothiazoles, also known as pseudosaccharins, are often vital structural units of biologically active systems and have important applications in major areas. Benzisothiazolyl and isothiazolyl derivatives are used in agriculture, as herbicides, fungicides, and pesticides.^{1,2} In medicine, benzisothiazole derivatives act as antibiotic agents,³ as phospholipase inhibitors in the treatment of hepatic diseases,⁴ as inhibitors of the human leukocyte elastase,^{5,6} and as selective blockers of the estrogen receptor, in the treatment of breast cancer.⁷ A new class of substituted benzisothiazolones has shown antiviral activity against retroviruses (e.g., HIV virus),⁸ and the first nonbenzoannelated 4-amino-2,3-dihydroisothiazole 1,1-dioxide, lacking a 3-oxo group, has recently been described and shows anti-HIV-1 activity.^{9,10}

Pseudosaccharyl ethers have particularly important synthetic uses as intermediate compounds for reductive cleavage of the C–O bond in phenols and alcohols.^{11–13} Much of the reactivity of these ethers can be ascribed to changes in bond lengths around the central C_{HAR}–O–C_A ether bonds (HAR = heteroaromatic ring and A = allyl, benzyl, naphthyl, or aryl group), caused by the powerful electron-withdrawing effect of the pseudosaccharyl ring system. The neat result of these electronic changes provides a molecular structure in which the originally strong C_A–O bond becomes easily cleavable. When the compounds are heated neat or in solution, this bond may then be broken, while the C_{HAR}–O bond becomes a double bond, affording the corresponding

N-allyl- or *N*-alkylbenzisothiazolones through Cope- or Chapman-like isomerizations, respectively.^{14–18}

The thermal isomerization of 3-methoxy-1,2-benzisothiazole 1,1-dioxide has been addressed recently.¹⁷ It was shown that its Chapman-type conversion into 2-methylbenzisothiazol-3-one 1,1-dioxide occurs in the melted phase and also in the crystalline phase. The mechanism was investigated on the basis of X-ray diffraction analysis and computational models.¹⁸ Results point to an energetic preference for a “quasi-simultaneous” intermolecular [1,3'] transfer of methyl, over an intramolecular mechanism.¹⁸

On the other hand, the thermal isomerizations of several 3-allyloxybenzisothiazoles have been studied in the melted phase and in solution,^{14–16} and the obtained results indicated that migration of the allyl group from O to N may proceed through both [1,3'] and [3,3'] mechanisms, the relative importance of each mechanism depending on various factors: structure of the allyl vinyl system (effect of substitution on the allylic moiety), polarity of the reaction medium, and temperature and time of reaction. The thermal behavior of the studied 3-allyloxybenzisothiazoles contrasts with that observed for the corresponding tetrazolyl derivatives,^{19–21} known to afford exclusively the [3,3'] isomers when heated, through a concerted mechanism similar to the symmetry-allowed general Cope rearrangement.^{22,23} For the allylsaccharyl ethers, it may be proposed that the [3,3'] isomers result from a concerted sigmatropic rearrangement, similar to that observed for allyloxytetrazoles. On the other hand, the [1,3'] isomers could result from a fragmentation–recombination mechanism or, alternatively, from an allowed concerted pseudopericyclic process similar to that observed in the rearrangement of allylic esters.^{24,25}

There are then still many open questions regarding the isomerization of allylsaccharyl ethers, which deserve further investigation. In the present paper, we report the results of our

* Corresponding author. E-mail: rfausto@ci.uc.pt.

[†] University of Coimbra.

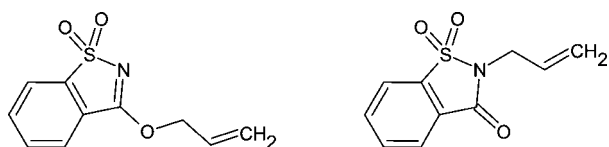
[‡] University of Buenos Aires.

[§] Jagiellonian University.

^{||} University of Algarve.

[⊥] Center for Research and Development in Food Cryotechnology.

SCHEME 1: Structures of 3-(Allyloxy)-1,2-benzisothiazole 1,1-Dioxide (ABID; left) and 2-Allyl-1,2-benzisothiazol-3(2H)-one 1,1-Dioxide (ABIOD; right)



studies on the thermal isomerization of 3-(allyloxy)-1,2-benzisothiazole 1,1-dioxide (ABID; Scheme 1) using a concerted methodological approach, in which temperature dependent infrared spectroscopy, differential scanning calorimetry, and polarized light thermomicroscopy were used, complemented by theoretical methods. The selection of the target compound was partially dictated by the fact that we have recently characterized in detail structurally and spectroscopically both the reactant molecule (ABID) and the isomerization product, 2-allyl-1,2-benzisothiazol-3(2H)-one 1,1-dioxide (ABIOD; Scheme 1),^{26,27} so that the present study can take advantage of the previously obtained information.

Experimental and Computational Methods

3-(Allyloxy)-1,2-benzisothiazole 1,1-dioxide (ABID) was synthesized by reaction of prop-2-en-1-ol with 3-chloro-1,2-benzisothiazole 1,1-dioxide (pseudosaccharyl chloride), in the presence of base, as described for the synthesis of other allyloxysaccharins.¹⁶ The required product was obtained as light yellow needles from ethanol (62% yield; mp 140 ± 0.1 °C; ¹H NMR (300 MHz, CDCl₃) δ , 5.05 (2H, d), 5.40–5.60 (2H, dd), 6.10–6.20 (1H, m), 7.70–7.80 (3H, m), 7.90 (1H, d); MS (CI) m/z 224 ([M + H]⁺), m/z 241 ([M + NH₄]⁺).

2-Allyl-1,2-benzisothiazol-3(2H)-one 1,1-dioxide (ABIOD) was obtained from ABID, by heating a neat sample at ca. 150 °C and keeping the sample at this temperature until all reactant had disappeared, as confirmed by thin layer chromatography (TLC) analysis (quantitative yield; mp 77–82 °C; ¹H NMR (300 MHz, CDCl₃): δ , 4.30–4.40 (2H, d), 5.20–5.35 (2H, m), 5.80–6.00 (1H, m), 7.70–7.80 (3H, m), 7.90 (1H, d); MS (CI) m/z 224 ([M + H]⁺, m/z 241 ([M + NH₄]⁺); MS (EI) m/z 197 ([M]⁺, 100%).

The infrared spectra, in the 500–4000 cm⁻¹ range, were recorded for the compound diluted in a KBr pellet, using a Bomem MB104 FT spectrometer, with 4 cm⁻¹ resolution, and a SPECAC variable temperature infrared cell connected to a digital controller (Shinho, MCD 530), which enables one to attain an accuracy in the temperature of ca. ± 1 °C. The temperature was measured directly at the sample holder by an iron/constantan (copper–nickel) J-type thermocouple. The sample compartment of the spectrometer was purged during all experiments by means of a constant flux of dry nitrogen, to avoid contamination from absorptions due to atmospheric water and CO₂.

Thermal studies were carried out in a differential scanning calorimetry (DSC) Perkin-Elmer DSC7, a power compensation calorimeter with a CCA7 cooling unit, over the temperature range 25–210 °C, with scanning rate 10 °C min⁻¹. Data acquisition and determination of the onset temperatures and transition enthalpies were performed with the Perkin-Elmer 1020 Series Thermal Analysis System Software. The samples were hermetically sealed in aluminum pans, and an empty pan was used as reference. No sample weight loss occurred in any experiment. A 20 mL min⁻¹ nitrogen purge was employed. Temperature calibration²⁸ was performed with high grade

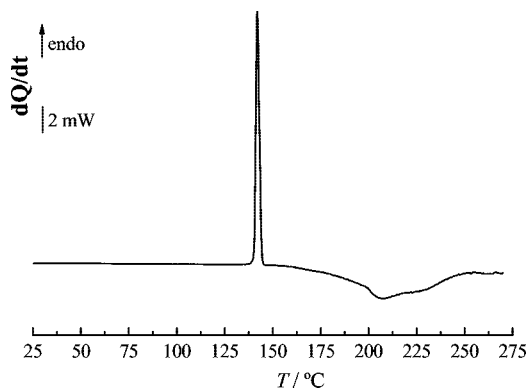


Figure 1. DSC curve of the first heating run of ABID: $m = 2.18$ mg; heating rate 10 °C min⁻¹.

standards, namely, biphenyl ($T_{\text{fus}} = 68.93 \pm 0.03$ °C) and zinc ($T_{\text{fus}} = 419.53$ °C), and verified with naphthalene ($T_{\text{fus}} = 80.20 \pm 0.04$ °C), benzoic acid ($T_{\text{fus}} = 122.35 \pm 0.02$ °C), and indium ($T_{\text{fus}} = 156.60$ °C). For heat calibration, the enthalpy of fusion of indium was used ($\Delta_{\text{fus}}H = 3286 \pm 13$ J mol⁻¹).²⁸

The hot stage/DSC video microscopy study was carried out by means of a Linkam DSC600 system. The optical equipment attached to the hot stage system consists of a DMRB Leica microscope fitted with polarized light facilities, to which a Sony CCD-IRIS/RGB video camera is attached. A Linkam system software with Real Time Video Measurement was used for image analysis. A small amount of the sample to be studied was placed in a glass crucible used as a cell, which was covered with a glass lid. Thermal cycles were followed by 200 \times magnification and the images obtained by combined use of polarized light and wave compensators. The thermal program for the microscope examination was run at 10 °C min⁻¹. Biphenyl and benzoic acid were used to confirm temperature accuracy.

All geometry optimizations and calculations of the infrared spectra were performed at the recommended²⁹ level of theory for pseudosaccharin compounds, DFT(B3LYP)/6-311++G-(3df,3pd),^{30,31} using the Gaussian 03 program package.³²

Results and Discussion

DSC and Polarized Light Thermomicroscopy Experiments. The thermal behavior of pure ABID was characterized by differential scanning calorimetry (DSC) between 25 and 275 °C. A typical DSC heating curve is presented in Figure 1.

The endothermic peak observed corresponds to the melting process, which occurs at $T_{\text{fus}} = 140.0 \pm 0.1$ °C ($n = 5$; where n is the number of determinations), the corresponding enthalpy, $\Delta_{\text{fus}}H$, being 25.6 ± 0.2 kJ mol⁻¹ ($n = 5$). The large exothermic peak observed between 150 and 260 °C is attributed to the ABID \rightarrow ABIOD isomerization. Note that it is clear from Figure 1 that this process takes place only in the melt. As discussed later on in this paper, the infrared studies also clearly confirm this conclusion. The measured enthalpy of the ABID \rightarrow ABIOD isomerization is equal to -45.1 ± 0.2 kJ mol⁻¹ ($n = 5$), thus being very similar to that obtained theoretically, at the DFT(B3LYP)/6-311++G(3df,3pd) level of approximation, for the isolated molecule: -49.3 kJ mol⁻¹.

Images obtained by thermomicroscopy during the heating process of ABID are shown in Figure 2. No transformation but the fusion of the compound is observed.

Very interestingly, on cooling the melt from 275 to 25 °C, neither DSC nor thermomicroscopy depicted any observable transformation. The samples were, then, kept at room temperature for 30 days and subsequently submitted to new experi-

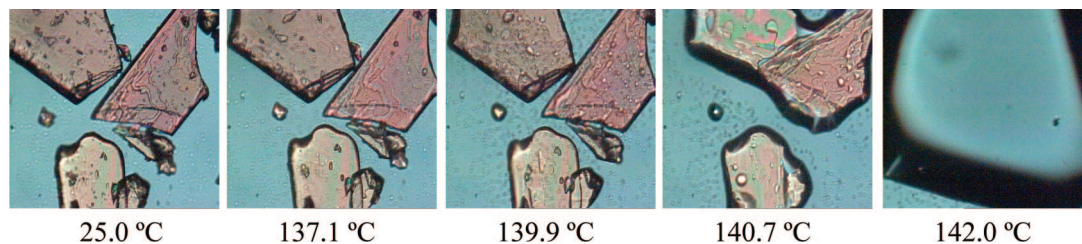


Figure 2. Fusion process of ABID observed by polarized light thermomicroscopy. Magnification 200 \times . Heating rate 10 $^{\circ}\text{C min}^{-1}$.

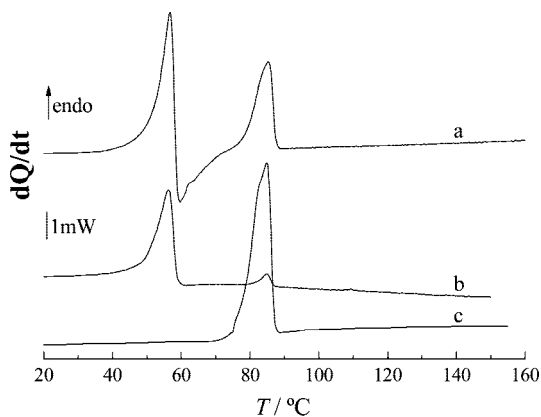


Figure 3. DSC heating curves of ABIOD samples prepared by annealing at room temperature the liquid obtained in the heating process of ABID: (a) and (b) one month; (c) one year; heating rate 10 $^{\circ}\text{C min}^{-1}$; (a) and (c) $m = 2.99$ mg; (b) $m = 2.18$ mg.

ments. As expected, the DSC heating curves of these samples revealed a completely different thermal behavior from that of the untreated ABID. Indeed, they represent the characteristic thermal behavior of ABIOD. Illustrative DSC curves are presented in Figure 3. They show two endothermic peaks, ascribable to fusion of different polymorphic species of ABIOD (Figure 3a, b). The peak observed at lower temperature (ca. 50 $^{\circ}\text{C}$) is assigned to the melting of a metastable phase of ABIOD; the one at higher temperature (ca. 80 $^{\circ}\text{C}$) corresponds to the fusion of the stable crystalline state. The metastable solid phase may either melt and stay as a liquid phase (Figure 3b; see also Figure 4 showing the thermomicroscopy results) or recrystallize to a more stable phase (Figure 3a). The metastable phase is kinetically preferred over the stable polymorph, and the amount of metastable phase formed and its rate of conversion to the stable phase depend on the specific sample, thus being impossible to predict a priori (in other terms, uncontrollable experimental variables, like defects on the pan surface, distribution of sample in the pan, etc., strongly influence the results). On the other hand, if the sample is kept for several months at room temperature, only the peak corresponding to the higher temperature transition is observed (Figure 3c). This peak exhibits some structure, pointing to a complex (multistep) fusion process, which was not further explored in this study.

The thermomicroscopy experiments also allowed us to characterize the morphology of the studied polymorphs of ABIOD as obtained from the melt. As seen in Figure 4, the metastable crystals are needles melting around 50 $^{\circ}\text{C}$, while the crystals of the stable polymorph are plate shaped.

Another interesting conclusion that can be extracted from Figure 1 is the fact that, although the ABID \rightarrow ABIOD isomerization does not take place before the melting of ABID, it appears to begin at temperatures only slightly above the melting temperature, though at a considerably slower rate. Figure 5 shows the results obtained when a sample of pure ABID was

submitted to several heating and cooling cycles between 25 and 160 $^{\circ}\text{C}$. Curves b and c in this figure clearly reveal that ABID has been partially converted to ABIOD, the concentration of ABIOD in the sample increasing with the number of cycles. This can be easily noticed by the relative areas of the endothermic peaks corresponding to melting of ABIOD (at ca. 70 $^{\circ}\text{C}$) and ABID and by the expected broadening and decrease of the melting temperatures originating from the simultaneous presence in the sample of the two compounds. As shown in the next section, the infrared studies were able to confirm that the ABID \rightarrow ABIOD conversion can take place at even lower temperatures in the melt (150 $^{\circ}\text{C}$).

Infrared Spectroscopy Experiments. In our previous infrared spectroscopic study of ABID, carried out for the matrix isolated compound and supported by extensive high level quantum chemical calculations,²⁶ it was shown that the monomer of this molecule can exist in five different conformational states, differing in the orientation of the allyl substituent. The most stable conformer was shown to be the TSk form, where the C–O–C–C and O–C–C=C dihedral angles were found to be 177.2 $^{\circ}$ and 124.2 $^{\circ}$, respectively. The infrared spectra of all conformers were found to be almost coincident.²⁶ Indeed, even for the compound isolated in cryogenic matrices (where as a general rule infrared bands are very narrow, with half-bandwidths typically of some tenths of cm^{-1} to a few cm^{-1}),³³ only a small number of bands could be assigned to individual conformers.²⁶ For the compound in the neat condensed phases, we can then easily discard the possibility of identification of spectroscopic features from individual conformers. On the other hand, for this type of compound, it has been shown that intermolecular interactions in the condensed phases are not strong enough to disturb significantly the intramolecular vibrational modes.¹⁷ This evidence rather simplifies the choice of the theoretical spectrum of ABID to be used as reference to help the analysis of the experimental data discussed in the present study. In fact, we could safely use the theoretically calculated infrared spectrum for the most stable conformer of ABID (the TSk form²⁶). A similar situation occurs for ABIOD. This compound does also have several low energy conformers differing in the orientation of the allylic fragment,²⁷ but the calculated infrared spectrum for its most stable conformer can also be used safely as a good approximation of the spectra of the neat condensed phases of the compound.

The selected reference theoretical spectra for ABID and ABIOD are shown in Figure 6 (spectra a and f, respectively). In this figure, the relevant experimental spectra showing the ABID \rightarrow ABIOD isomerization are also presented. Spectrum b is the room temperature spectrum of ABID in the crystalline state (in KBr pellet), which agrees very nicely with the calculated spectrum for this compound. Spectrum c was obtained at 150 $^{\circ}\text{C}$, immediately after the fusion of the compound. It essentially duplicates the spectrum of the crystalline phase, only showing the expected characteristic band broadening, mainly associated with the increase of the local inhomogeneity and more

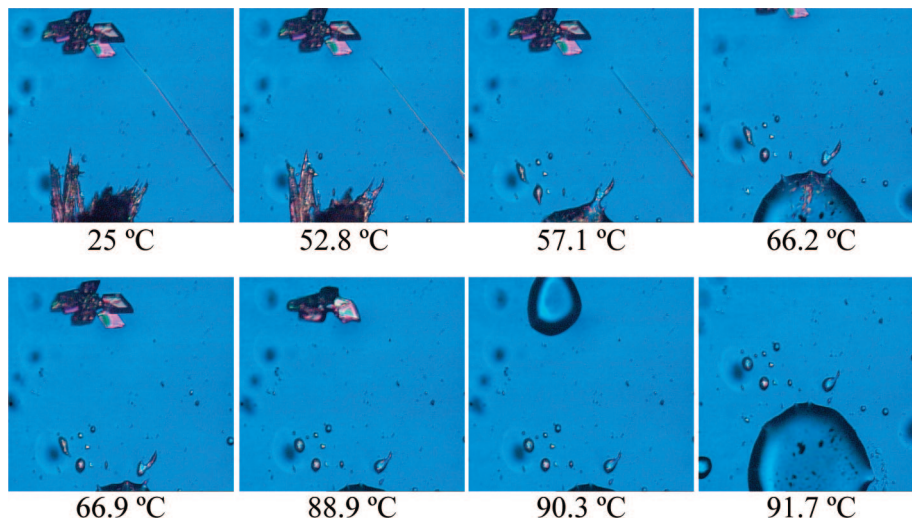


Figure 4. Fusion process of ABIOD observed by polarized light thermomicroscopy. Samples prepared by annealing at room temperature, for 30 days, the liquid obtained in the heating process of ABID. Magnification 200 \times . Heating rate 10 $^{\circ}\text{C min}^{-1}$.

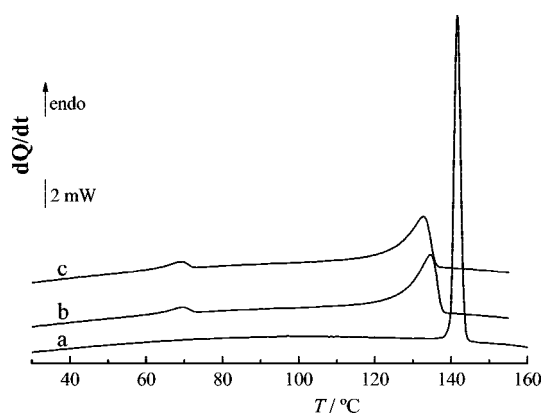


Figure 5. DSC heating curves obtained in heating/cooling cycles of ABID: (a) first heating run; (b) second heating run; (c) third heating run; $m = 2.64$ mg; heating rate 10 $^{\circ}\text{C min}^{-1}$.

important contributions from higher energy conformers. Spectrum d was also obtained at 150 $^{\circ}\text{C}$, but after 92 min of annealing, and shows partial conversion of ABID into ABIOD. Particularly useful to follow this conversion is the 1800–1500 cm^{-1} spectral region, where ABID gives rise to two main bands, at ca. 1615 and 1557 cm^{-1} (ascribed to a ring stretching mode and the C=N stretching vibration, respectively²⁶), and ABIOD gives rise to the characteristic carbonyl stretching mode band at ca. 1730 cm^{-1} . Finally, spectrum e in Figure 6 was obtained at 220 $^{\circ}\text{C}$, after the ABID \rightarrow ABIOD isomerization has been completed. This spectrum fits nicely the calculated spectrum for ABIOD (spectrum f).

In the Supporting Information (Tables S1 and S2), the proposed assignments for the spectra of ABID and ABIOD in the neat condensed phases are provided. Note that the spectra of the polymorphic phases of ABIOD were found to be very similar, the 1400–1100 cm^{-1} spectral range (Figure 7) being the one where the two spectra exhibit the most relevant differences. The two SO_2 stretching vibrations and several modes associated with the allyl fragment [e.g., νCH_2 , twCH_2 , $\delta(\text{=CH})$, $\nu(\text{=CH}_2)$] are the main contributors to this spectral region (together with the $\nu\text{C-N}$ stretching), which seems to indicate that the crystalline structures differ mainly in the relative orientation of the allylic and SO_2 groups, i.e., point to different degrees of conformational mobility of the allylic fragment in the crystals.

The temperature dependence of the rate of the ABID \rightarrow ABIOD isomerization process was investigated spectroscopically

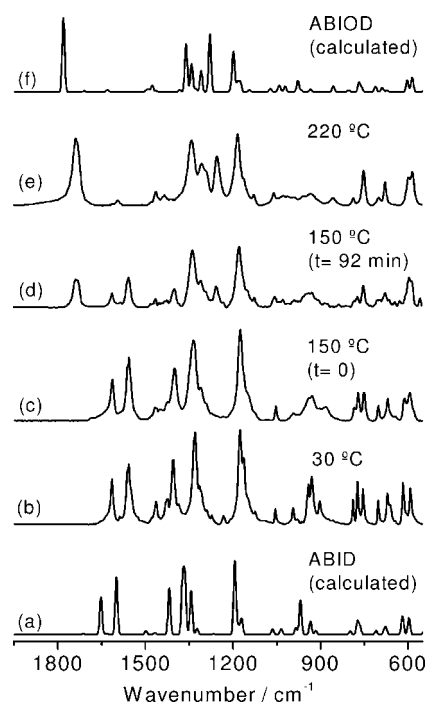


Figure 6. (a) Calculated [DFT(B3LYP)/6-311++G(3df,3pd)] infrared spectrum for ABID; (b) room temperature (30 $^{\circ}\text{C}$) infrared spectrum of polycrystalline ABID in KBr pellet; (c, d) infrared spectra at 150 $^{\circ}\text{C}$, obtained during the heating of the ABID sample: spectrum c was obtained immediately after the sample has attained 150 $^{\circ}\text{C}$, while spectrum d was obtained after annealing the sample at this temperature for 92 min; (e) infrared spectrum at 220 $^{\circ}\text{C}$, obtained during the heating of the ABID sample; (f) calculated [DFT(B3LYP)/6-311++G(3df,3pd)] infrared spectrum for ABIOD.

within the 135–240 $^{\circ}\text{C}$ temperature range. Figure 8 shows the normalized (to unity) reactant concentration decays determined from the integrated intensities of the bands in the 1610–1550 cm^{-1} wavenumber range ascribed to ABID. For temperatures below the melting point of ABID, no reaction was observed. For temperatures above ca. 150 $^{\circ}\text{C}$, the reaction starts to take place following a kinetics described by a single exponential decay, in agreement with the occurrence of a single process of intramolecular nature (see Table 1, for obtained rate constants). In this regard, the observed kinetics is distinctly different from that previously determined for the Chapman-type isomerization

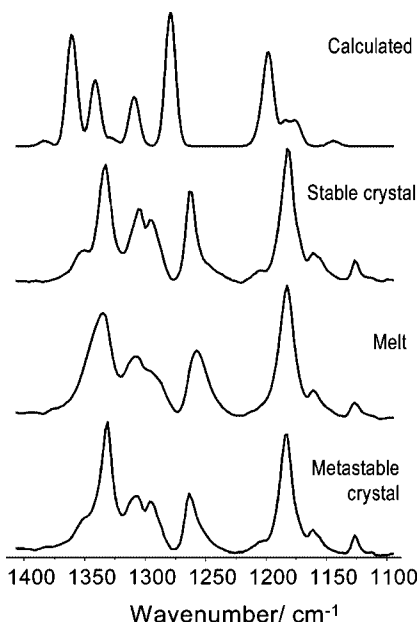


Figure 7. 1400–1100 cm^{-1} spectral range of the IR spectra of ABIOD. From bottom to top: spectra of the metastable crystal, melt, stable crystal, and calculated [DFT(B3LYP)/6-311++G(3df,3pd)] for the isolated molecule. The stable crystal was produced after synthesis of the compound and annealing at room temperature for 1 year; the melted phase was obtained by heating to 220 °C the stable crystalline phase; the spectrum of the metastable phase was obtained immediately after crystallization of the molten compound.

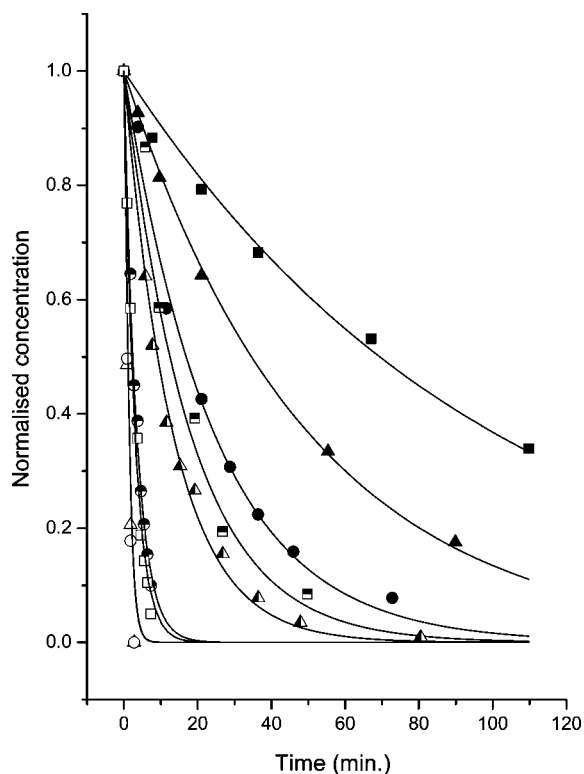


Figure 8. Normalized (to unity) reactant concentration decays obtained from the integrated intensities of the ABID infrared bands in the 1610–1550 cm^{-1} wavenumber range. T (°C): ■ 150, ▲ 160, ● 170, □ 180, △ 190, ● 200, □ 210, △ 230, ○ 240.

of the analogous alkyloxy substituted pseudosaccharin, 3-methoxy-1,2-benzisothiazole 1,1-dioxide, that was found to be intermolecular and to follow a sigmoidal-type Bawn kinetics,³⁴ compatible with the occurrence of that process in both the solid

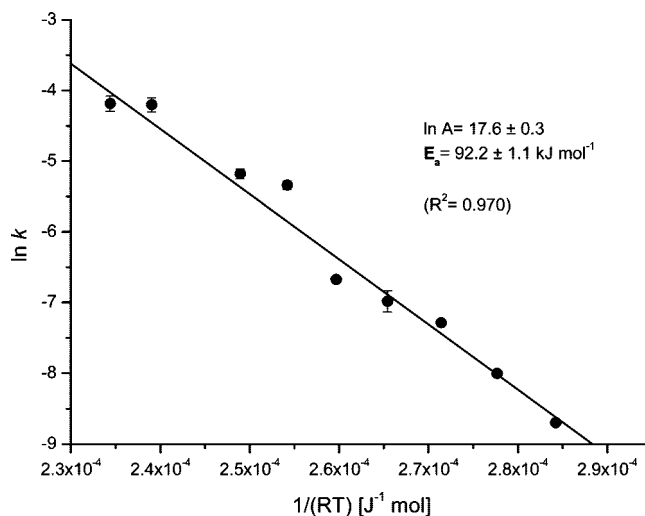


Figure 9. Arrhenius plot of $\ln k$ vs $1/(RT)$, yielding the activation energy (E_a) for the ABID \rightarrow ABIOD isomerization process.

TABLE 1: Rate Constants for the ABID \rightarrow ABIOD Thermal Isomerization at Different Temperatures

T (°C)	k (s^{-1}) $\times 10^4$
150	1.66 ± 0.06
160	3.34 ± 0.05
170	6.85 ± 0.23
180	9.28 ± 1.40
190	12.6 ± 0.4
200	48.0 ± 2.9
210	56.1 ± 3.8
230	149.4 ± 14.9
240	152.0 ± 16.5

and the melted phases^{17,18} (MBID \rightarrow MBIOD transformation has been addressed in detail in refs 17 and 18, where a quasi-synchronous intermolecular double methyl group transfer was shown to be energetically favored in relation to the intramolecular process). Furthermore, the experimental evidence also indicates that under the experimental conditions used, and contrarily to what was observed in solution, where both [1,3'] and [3,3'] rearrangements were shown to take place simultaneously,¹⁵ only one of these processes occurs.

The Arrhenius plot shown in Figure 9 allowed obtaining of the activation energy of the ABID \rightarrow ABIOD isomerization process, which was found to be $92.2 \pm 1.1 \text{ kJ mol}^{-1}$. This value is very similar to those measured or estimated theoretically for concerted sigmatropic rearrangements in similar compounds {e.g., in allylcyclopentenyl ethers³⁵ $71.1\text{--}87.9 \text{ kJ mol}^{-1}$ (in benzene), cyanosubstituted allylvinyl ethers³⁶ $92.0\text{--}117.2 \text{ kJ mol}^{-1}$ (in diethyl ether), 5-allyloxy-1-phenyltetrazoles²⁰ $69.0\text{--}92.0 \text{ kJ mol}^{-1}$ (in DMSO) or $82.0\text{--}103.8 \text{ kJ mol}^{-1}$ (in 1,1,2,2-tetrachloroethane)}, strongly suggesting that the observed reaction corresponds in fact to the symmetry-allowed general [3,3'] Cope rearrangement. Another indication pointing to the same conclusion comes from theoretical results. Nori-Sharg et al.³⁷ have shown that the HOMO–LUMO energy gap correlates with the activation barrier of allylic hetero Cope rearrangements, and the larger the energy gap, the larger the activation barrier. In their studies, those authors correlated energy barriers within 163 and 200 kJ mol^{-1} with a HOMO–LUMO energy gap of ca. 7 eV, and within 97–121 kJ mol^{-1} with a HOMO–LUMO gap of ca. 5 eV. For ABID, the HOMO–LUMO energy gap was calculated to be 5.3 eV, thus closely obeying the Nori-Sharg correlation. The study of the isomerization reaction of selected

isotopically substituted analogues of ABID is required, however, to firmly confirm this conclusion.

Conclusions

The isomerization of the neat pseudosaccharyl ether, 3-(allyloxy)-1,2-benzisothiazole 1,1-dioxide (ABID), to the corresponding *N*-allyl pseudosaccharin (ABIOD) was studied by infrared spectroscopy, DSC, and thermomicroscopy, complemented by theoretical calculations undertaken at the DFT-(B3LYP)/6-311++G(3df,3pd) level of approximation. It was shown that the process occurs only above the melting point of the reactant (140.0 ± 0.1 °C). The reaction was found to obey a first order kinetics, showing single exponential decay isotherms, with an activation energy of 92.2 ± 1.1 kJ mol⁻¹. These data are in agreement with the expected intramolecular and concerted nature of the reaction, and then consistent with the process corresponding to a sigmatropic reaction (symmetry-allowed general [3,3'] Cope rearrangement).

In the temperature range investigated, ABIOD was found to exhibit polymorphism. Cooling of the molten compound leads to the production of a metastable crystalline form (melting temperature: ca. 50 °C), which upon annealing at room temperature might be transformed to the stable crystalline phase. ABID shows a single crystalline variety. The infrared spectra of the observed neat condensed phases of the two compounds were assigned on the basis of comparison with results of theoretical calculations and taking into account previous experimental data obtained for these compounds isolated in cryogenic inert matrices.^{26,27}

Acknowledgment. The research was supported by the Portuguese *Fundação para a Ciência e a Tecnologia* (Projects PTDC/QUI/71203/2006, PTDC/QUI/67674/2006, and FCT/MINCYT/SN/2007) and the Argentinean Agency for the Promotion of Science and Technology (Project PICT 2006/00068). Calculations were partially done at the Academic Computer Center "Cyfronet", Krakow, Poland (Grant KBN/SGI_ORIGIN 2000/UJ/044/1999), which is acknowledged for computing time. A.G.-Z. is a member of the research career Conicet (National Research Council, Argentina).

Supporting Information Available: Band assignments for the infrared spectra of the observed neat condensed phases of ABID and ABIOD (Tables S1 and S2). This material is available free of charge via the Internet at <http://pubs.acs.org>.

References and Notes

- Otten, M.; von Deyn, W.; Engel, S.; Hill, R.; Kardorff, U.; Vossen, M.; Plath, P. Isoxazole-4-yl-benzoyl derivatives and their use as herbicides. Patent WO9719076, Internationale Anmeldung Veröffentlicht nach dem Vertrag über die Internationale Zusammenarbeit auf dem Gebiet des Patentwesens. Weltorganisation für Geistiges Eigentum, 1997.
- Wepplo, P. J.; Rampulla, R. A.; Heffernan, G. D.; Cosette, M. V.; Diehl, R. E.; Fiordeliso, J. J.; Haley, G. J.; Guaciario, M. A. Herbicidal 3-heterocyclic substituted benzisothiazole and benzisoxazole compounds. Patent WO0179203, Internationale Anmeldung Veröffentlicht nach dem Vertrag über die Internationale Zusammenarbeit auf dem Gebiet des Patentwesens. Weltorganisation für Geistiges Eigentum, 2004.
- Gravestock, M. B. Bicyclic heterocyclic substituted phenyl oxazolidinone anti-bacterials, and related compositions and methods. Patent WO/1999/10342, Internationale Anmeldung Veröffentlicht nach dem Vertrag über die Internationale Zusammenarbeit auf dem Gebiet des Patentwesens. Weltorganisation für Geistiges Eigentum, 1999.
- Eacho, P. I.; Foxworthy-Mason, P. S.; Lin, H.-S.; Lopez, J. E.; Mosior, M.; Richett, M. E. Benzisothiazol-3-one-carboxylic acid amides as phospholipase inhibitors. Patent WO/2004/094394, Internationale Anmeldung Veröffentlicht nach dem Vertrag über die Internationale Zusammenarbeit auf dem Gebiet des Patentwesens. Weltorganisation für Geistiges Eigentum, 2004.

- Hlasta, D. J.; Bell, M. R.; Court, J. J.; Cundy, K. C.; Desai, R. C.; Ferguson, E. W.; Gordon, R. J.; Kumar, V.; Maycock, A. L.; Subramanyam, C. *Bioorg. Med. Chem. Lett.* **1995**, *5*, 331.
- Subramanyam, C.; Bell, M. R.; Ferguson, E.; Gordon, R. G.; Dunlap, R. P.; Franke, C.; Mura, A. J. *Bioorg. Med. Chem. Lett.* **1995**, *5*, 319.
- Wang, L. H.; Yang, X. Y.; Zhang, X.; Mihalic, K.; Fan, Y. X.; Xiao, W.; Zack Howard, O. M.; Appella, E.; Maynard, A. T.; Farrar, W. L. *Nat. Med.* **2004**, *10*, 40.
- Sharmeen, L.; McQuade, T.; Heldsinger, A.; Gogliotti, R.; Domagala, J.; Gracheck, S. *Antiviral Res.* **2001**, *49*, 101.
- Marco, J. L.; Ingate, S. T.; Chinchon, P. M. *Tetrahedron* **1999**, *55*, 7625.
- Marco, J. L.; Ingate, S. T.; Jaime, C.; Bea, J. *Tetrahedron* **2000**, *56*, 2523.
- Araújo, N. C. P.; Brigas, A. F.; Cristiano, M. L. S.; Frijia, L. M. T.; Guimarães, E. M. O.; Loureiro, R. M. S. *J. Mol. Catal., A* **2004**, *215*, 113.
- Frijia, L. M. T.; Cristiano, M. L. S.; Guimarães, E. M. O.; Martins, N. C.; Loureiro, R. M. S.; Bickley, J. J. *Mol. Catal. A: Chem.* **2005**, *242*, 241.
- Brigas, A. F.; Johnstone, R. A. W. *J. Chem. Soc., Perkin Trans. 1* **2000**, 1735.
- Barkley, J. V.; Cristiano, M. L. S.; Johnstone, R. A. W.; Loureiro, R. M. S. *Acta Crystallogr., Sect. C* **1997**, *53*, 383.
- Cristiano, M. L. S.; Brigas, A. F.; Johnstone, R. A. W.; Loureiro, R. M. S.; Pena, P. C. A. *J. Chem. Res., Synop.* **1999**, 704.
- Araújo, N. C. P.; Barroca, P. M. M.; Bickley, J. F.; Brigas, A. F.; Cristiano, M. L. S.; Johnstone, R. A. W.; Loureiro, R. M. S.; Pena, P. C. A. *J. Chem. Soc., Perkin Trans. 1* **2002**, 1213.
- Almeida, R.; Gómez-Zavaglia, A.; Kaczor, A.; Cristiano, M. L. S.; Eusébio, M. E. S.; Maria, T. M. R.; Fausto, R. *Tetrahedron* **2008**, *64*, 3296.
- Kaczor, A.; Proniewicz, L.; Almeida, R.; Gómez-Zavaglia, A.; Cristiano, M. L. S.; Matos Beja, A. M.; Ramos Silva, M.; Fausto, R. *J. Mol. Struct.* **2008**, *892*, 343.
- Cristiano, M. L. S.; Johnstone, R. A. W.; Price, P. J. *J. Chem. Soc., Perkin Trans. 1* **1996**, 1453.
- Cristiano, M. L. S.; Johnstone, R. A. W. *J. Chem. Soc., Perkin Trans. 2* **1997**, 489.
- Cristiano, M. L. S.; Johnstone, R. A. W. *J. Chem. Res.* **1997**, 164.
- Woodward, R. B.; Hoffmann, R. *The Conservation of Orbital Symmetry*; Verlag Chemie, GmbH: Weinheim, 1970.
- Ito, H.; Tagushi, T. *Chem. Soc. Rev.* **1999**, *28*, 43.
- Zipse, H. H. *J. Chem. Soc., Perkin 2* **1996**, *9*, 1797.
- Birney, D. M.; Xu, X.; Ham, S. *Angew. Chem., Int. Ed.* **1999**, *38*, 189.
- Gómez-Zavaglia, A.; Kaczor, A.; Almeida, R.; Cristiano, M. L. S.; Fausto, R. *J. Phys. Chem. A* **2008**, *112*, 1762.
- Gómez-Zavaglia, A.; Kaczor, A.; Coelho, D.; Cristiano, M. L. S.; Fausto, R. *J. Mol. Struct.*, in press.
- Sabbah, R.; Wu, A. X.; Chickos, J. S.; Leitão, M. L. P.; Roux, M. V.; Torres, L. A. *Thermochim. Acta* **1995**, *331*, 93.
- Kaczor, A.; Almeida, R.; Gómez-Zavaglia, A.; Cristiano, M. L. S.; Fausto, R. *J. Mol. Struct.* **2008**, *876*, 77.
- Becke, A. D. *Phys. Rev. A* **1988**, *38*, 3098.
- Lee, C. T.; Yang, W. T.; Parr, R. G. *Phys. Rev. B* **1988**, *37*, 785.
- Frisch, M. J.; Trucks, G. W.; Schlegel, H. B.; Scuseria, G. E.; Robb, M. A.; Cheeseman, J. R.; Montgomery, J. A., Jr.; Vreven, T.; Kudin, K. N.; Burant, J. C.; Millam, J. M.; Iyengar, S. S.; Tomasi, J.; Barone, V.; Mennucci, B.; Cossi, M.; Scalmani, G.; Rega, N.; Petersson, G. A.; Nakatsuji, H.; Hada, M.; Ehara, M.; Toyota, K.; Fukuda, R.; Hasegawa, J.; Ishida, M.; Nakajima, T.; Honda, Y.; Kitao, O.; Nakai, H.; Klene, M.; Li, X.; Knox, J. E.; Hratchian, H. P.; Cross, J. B.; Bakken, V.; Adamo, C.; Jaramillo, J.; Gomperts, R.; Stratmann, R. E.; Yazyev, O.; Austin, A. J.; Cammi, R.; Pomelli, C.; Ochterski, J. W.; Ayala, P. Y.; Morokuma, K.; Voth, G. A.; Salvador, P.; Dannenberg, J. J.; Zakrzewski, V. G.; Dapprich, S.; Daniels, A. D.; Strain, M. C.; Farkas, O.; Malick, D. K.; Rabuck, A. D.; Raghavachari, K.; Foresman, J. B.; Ortiz, J. V.; Cui, Q.; Baboul, A. G.; Clifford, S.; Cioslowski, J.; Stefanov, B. B.; Liu, G.; Liashenko, A.; Piskorz, P.; Komaromi, I.; Martin, R. L.; Fox, D. J.; Keith, T.; Al-Laham, M. A.; Peng, C. Y.; Nanayakkara, A.; Challacombe, M.; Gill, P. M. W.; Johnson, B.; Chen, W.; Wong, M. W.; Gonzalez, C.; Pople, J. A. Gaussian 03, revision C.02; Gaussian, Inc.: Wallingford, CT, 2004.
- Low Temperature Molecular Spectroscopy*; Fausto, R., Ed.; NATO-ASI Series C483; Kluwer Inc.: Amsterdam, The Netherlands, 1996.
- Bawn, C. E. H. The Decomposition of Organic Solids. Chapter 10 in *Chemistry in the Solid State*; Garner, W. E., Ed.; Butterworths: London, 1955.
- Coates, R. M.; Rogers, B. D.; Hobbs, S. J.; Peck, D. R.; Curran, D. P. *J. Am. Chem. Soc.* **1987**, *109*, 1160.
- Burrows, C. J.; Carpenter, B. K. *J. Am. Chem. Soc.* **1981**, *103*, 6983.
- Nori-Sharg, D.; Shiroudi, A.; Oliyai, A. R.; Deyhimi, F. *J. Mol. Struct. (THEOCHEM)* **2007**, *824*, 1.